

Robotics design challenge (MATLAB/SIMULINK)

Jiaqi, Yao. Ruixin, Zhan. Xuzhao, Zhang. Xiaoyu, Zhang

March 31, 2023

Abstract

1 Introduction

Our product is a type of mechanical equipment used for automated welding. Our robotic arm can be widely used in various welding operations in the manufacturing industry, including automotive manufacturing, aerospace, construction, and manufacturing.

Our product has many advantages. Firstly, it can improve production efficiency and quality by reducing the negative impact of human factors on production through automated welding operations. Secondly, it can reduce the danger of the work environment.

In summary, the four-arm welding robot is an efficient and accurate welding device with many advantages. It will become an important part of automated production in the manufacturing industry, providing a reliable solution for various production operations.

2 Task 1

2.1 Originality and uniqueness of the robot

Although a two-armed robot will be able to reach the required working space, it will suffer from imprecise movements and be prone to damage. And it cannot be adapted to other work types, increasing costs.

After discussion and doing some references, our group decide to make our robot arm as a four-arm robot and define the robot arms and joints, because there are some advantages of four-arm robot: better accuracy and stability of the movement; bigger working arrangement; better loading allowance; better collaboration.

And there are also some unique assessments of our four-robot arms can meet:

- The welding robot arm allows for more precise control of welding position and angle.
- Compared to manual welding, welding robots can automate welding work, thereby increasing productivity and reducing labor costs.
- To prevent clashes between arms and joints, we perform kinematic analysis to determine the minimum spacing and range of movement between joints and robot arms, and use MATLAB simulations to ensure collision-free operation with exact arm and joint parameters.
- After researching robot design, we consider working arrangement, stability, and operability. To achieve precise welding in a specific area, we define parameters for all arms and joints.

2.2 Property of all the arms and the joints

We have designed 4 joints for the robot, 2 of which are revolute type and 2 are prismatic type. At the same time, there are four corresponding robotic arms, whose parameters are shown in the Table 2.1 and Table 2.2

Name	Body Mass (kg)	Center of mass	Inertia (I_{xx} I_{yy} I_{zz}) ($kg \cdot m^2$)
R1	10	(0 0 0)	(0.27 0.27 0.8)
R2	10	(0 0 0)	(0.27 0.27 0.8)
P1	1.5	(0 0 0)	(0.07 0.07 0.07)
P2	1.5	(0 0 0)	(0.07 0.07 0.07)
Tool	1.2	(0 0 0)	(0.002 0.002 0.004)

Table 2.1: Experiment parameters

Joint	Type	Position Limit (rad & m)	Joint Axis
1	revolute	$[-5\frac{\pi}{180}, 5\frac{\pi}{180}]$	[0 0 1]
2	revolute	$[-30\frac{\pi}{180}, 30\frac{\pi}{180}]$	[0 1 0]
3	prismatic	$[-0.5, 0.5]$	[1 0 0]
4	prismatic	$[-1, 1]$	[0 1 0]
Fixed	revolute	N/A	N/A

Table 2.2: Experiment parameters

Figure 2.1 is a schematic diagram of the robot in MATLAB.

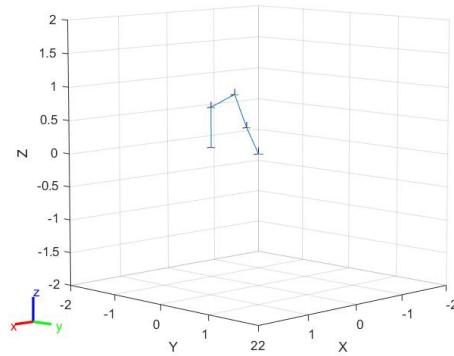


Figure 2.1: Force vs deformation and total moment diagram

2.3 Collision discussion

Our designed robot is free from collisions. In most cases, collisions occur on the two arms of the rotating joints whose rotation angle is greater than $\pm 90^\circ$. For our designed robot, the total range of

motion for the two movable joints is $\pm 35^\circ$, so there is no collision. Additionally, the animation of the robot's movement trajectory can be viewed in the dynamic image in Figure 8.

3 Task 2: The Workspace

Figure 3.1 shows the robot's workspace in Task 1. The robot can work with precision within this workspace and also carry out certain tasks outside the range.

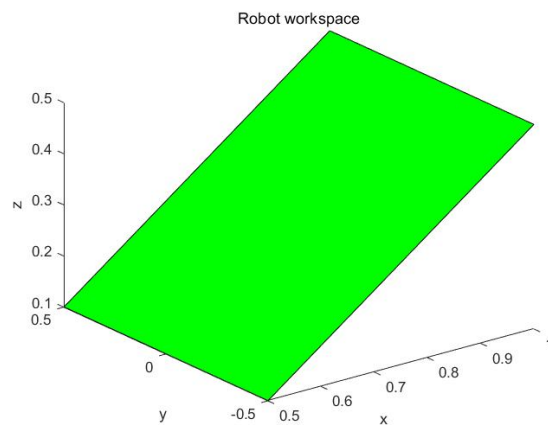


Figure 3.1: Robot's Workspace

4 Task 3: The robot's kinematic diagram

Figure 4.1 the drawing of the kinematic diagram using the Denavit-Hartenberg frame rules for the robot designed in task 1.

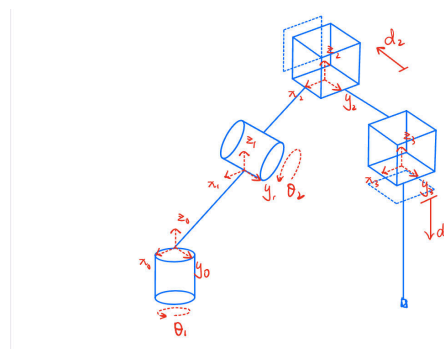


Figure 4.1: The robot's kinematic diagram

5 Task 4: Simulink and Simulation

5.1 Simulink

Figure 5.1 shows a schematic of Simulink.

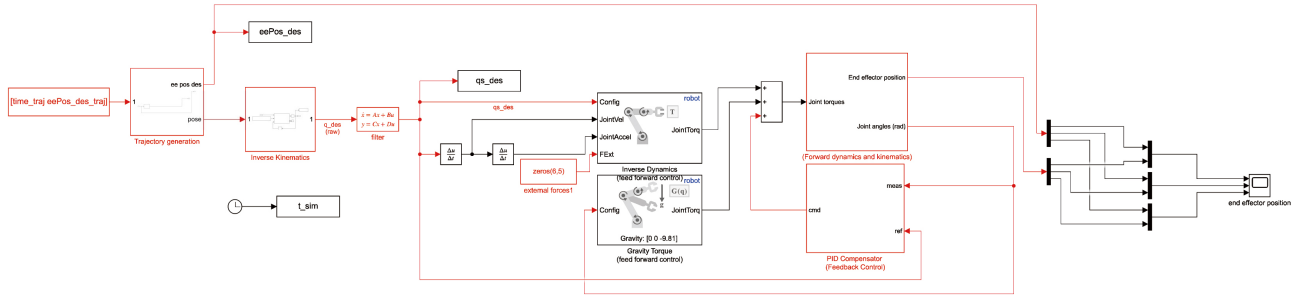


Figure 5.1: The Simulink

Tidy of the model

To ensure aesthetic appeal, a modular design approach was adopted, where different modules represent different functionalities, thereby making the overall model's operation flow appear clear and concise.

Trajectory generation

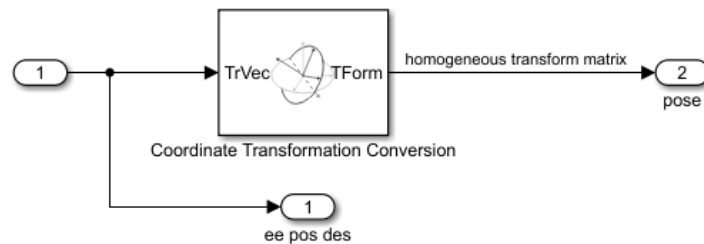


Figure 5.2: The Denevit-Hartenberg frame

We first calculate the path coordinate points and time series from the code, and use them as input parameters for trajectory calculation. Through trajectory calculation as shown in Figure 5.2, we can obtain the expected end-effector position and obtain motion trajectory data applicable to each

point after coordinate transformation (which records the three-dimensional coordinate points of the path every 0.01 seconds).

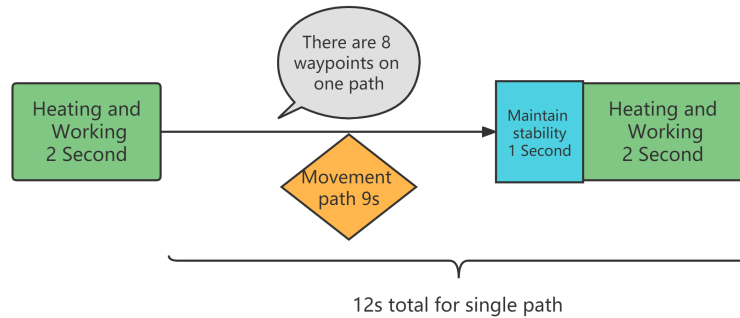


Figure 5.3: plastic modules of rectangular section

Figure 5.3 is a flowchart of the process we use to compute the trajectory of the robot's end effector position. First, we divide the rectangle required for the task into four line segments. For each line segment, we divide it into 9 equally long segments, and expect the robot to take 9 seconds to move along it. After that, the robot needs to spend 1 second for stabilization, followed by 2 seconds of welding work at the work point.

Inverse kinematics

In the inverse kinematics module, we use the expected end-effector position as input, as shown in Figure 5.4, and calculate the expected joint angles using inverse kinematics. The output is a matrix containing time-series data, which records the rotation angles of different joints of the robotic arm every 0.01 seconds.

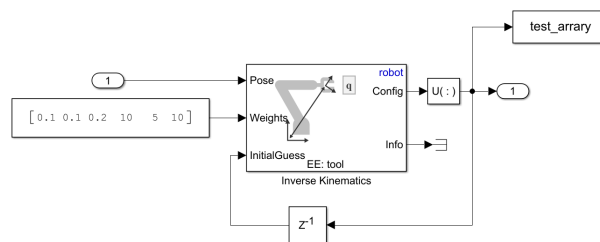


Figure 5.4: plastic modules of rectangular section

Inverse dynamics

Inverse dynamics is to calculate the forces or torques that are required to produce a desired motion of a robotic system. The technique involves using the system's equations of motion to determine the forces or torques required to generate a desired trajectory or motion. As shown in Figure 5.5, the input parameter in this part is the coordinate data of each sampling point calculated by the inverse kinematics. By weighting and differentiating the data, the required angular velocity and angular acceleration can be obtained. Then, the obtained data is imported into the inverse dynamics module for calculation, and the result is the torque required for each joint at each sampling point.

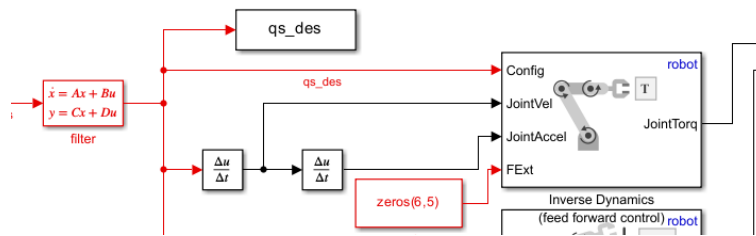


Figure 5.5: plastic modules of rectangular section

Gravity

In this part, the torque generated by gravity is added as a vector to the torque required by each joint calculated by the inverse dynamics module, and the combined torque vector is passed to the next module to simulate the deviation that may occur in the actual robot arm. The process is shown in Figure 5.6.

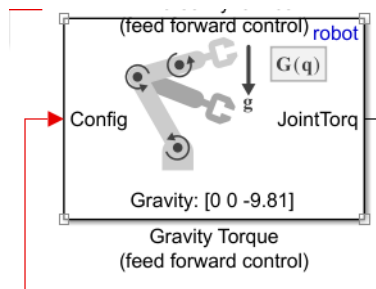


Figure 5.6: plastic modules of rectangular section

Forward dynamics and kinematics

Figure 5.7 shows the forward kinematics and dynamics module, in which the actual position and orientation of the end-effector can be calculated based on the actual joint angles obtained by considering the different torques inputted to each joint.

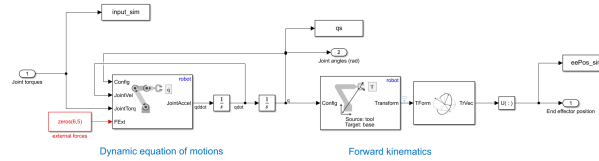


Figure 5.7: plastic modules of rectangular section

5.2 PID design

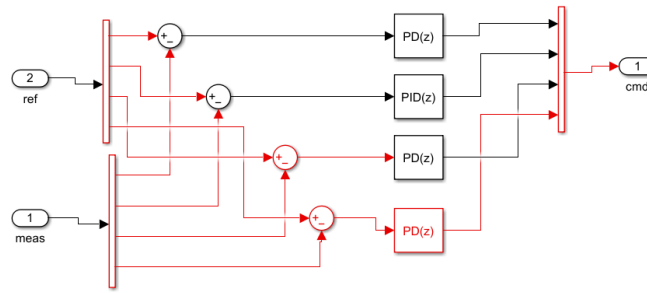


Figure 5.8: plastic modules of rectangular section

In the PID control module, as shown in Figure 5.8, we subtract the desired data from the actual data to obtain the error value, which is then used for PID calculation. We noticed that joints 1, 3, and 4 only use PD controllers because these three joints require a fast response speed and low overshoot, and have lower requirements for steady-state error. For joint 2, which uses a PID controller, it is sensitive to steady-state error due to its rotation around the y-axis. Although there may be difficulty in tuning, we successfully completed the debugging process.

5.3 Results

Finally, set the end effector positions and the desired end effector positions as the input, draw the plot with their x y z positions followed by the time respectively.

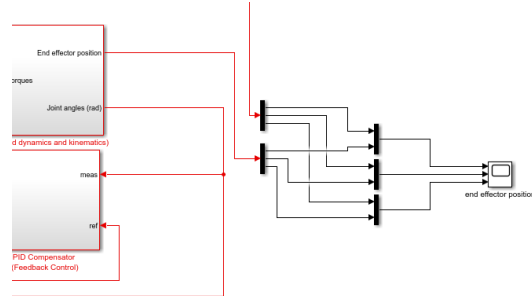


Figure 5.9: plastic modules of rectangular section

Input torque

As shown in the figure below, this is the torque figure of each joint required for the robot during operation. By observing the figure, it can be found that, except for the initial instability during startup, we only need less than $30 N \cdot m$ of torque to drive the robot to complete the welding task.

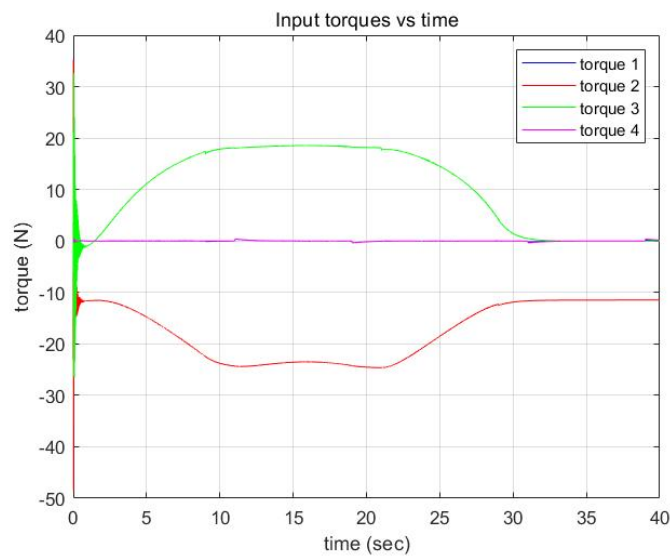


Figure 5.10: plastic modules of rectangular section

Joint angle

As we can see in the 'joint angle error' plot.

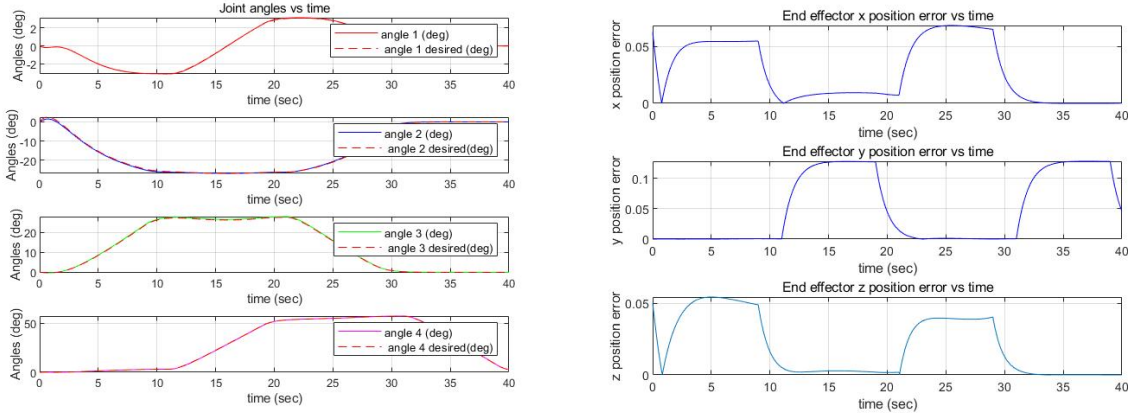


Figure 5.11: plastic modules of rectangular section

The error of joint1 angle does not exceed the limit of 10^{-3} , but it fluctuates throughout the process; The error of joint2 angle is the largest, and it nearly reaches 0.02, the error tends to be stable except for large fluctuations at the peak throughout the process; Both the maximum error of joint3 angle and joint4 angle are below $5 \cdot 10^{-3}$, but joint3 angle error are steady increase to the maximum error, and remain stable on the maximum angle error; as for joint4 angle, there is almost no error in the first ten seconds, and there is always a period of stability after the changes of the error. Overall, the errors are small and will not have a significant impact on the operation of the robot.

End Effector Position

As we can see in the 'end effector position error' plot, the maximum error in end effector position on the x and z axes is below 0.05, while the maximum error on the y axis is slightly over 0.10. The errors in the x and z axes fluctuate simultaneously, while the error in the y axis gradually increases as the errors in the former axes begin to decrease. There is a small amount of error throughout the entire process, but it is not significant. It has almost no impact in reality.

6 Conclusion

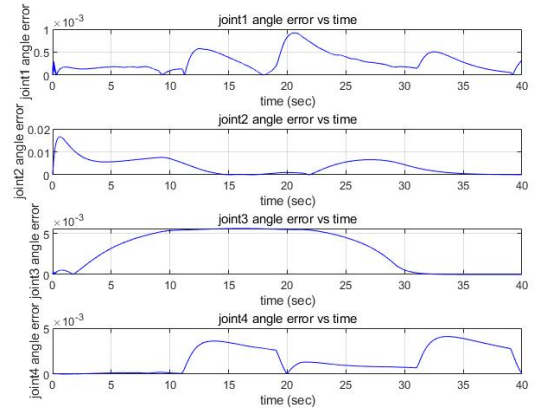
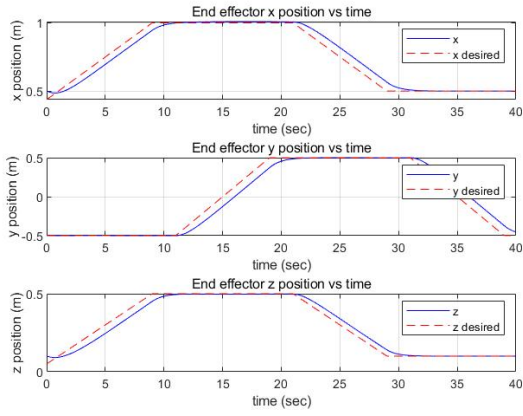


Figure 5.12: plastic modules of rectangular section

References